MICROIMAGING INFRARED SPECTROSCOPY FOR CHARACTERIZATION OF MARTIAN METEORITE COMPOSITIONAL DIVERSITY. J. K. Miura[1], B. L. Ehlmann[1,2], R. Greenberger[1], E. Cutts[3]. [1]Division of Geological and Planetary Sciences, California Institute of Technology, Pasadena, CA [2]Jet Propulsion Laboratory, California Institute of Technology, Pasadena, CA [3]University of Southern Denmark, Odense, Denmark (jmiura@caltech.edu)

Introduction: The Meteoritical Bulletin Database currently lists 247 meteorites with a Martian origin, representing 139 unique falls. Although these meteorites sample Martian history from 4.4 Ga to 170 Ma, there is a bias toward younger, more coherent igneous samples that can survive launch and delivery from the Martian surface [1]. Martian meteorites provide the opportunity to conduct laboratory analyses that complement remotely sensed and in-situ data collected on Mars. Characterizing how grain-scale petrologic observations of Martian meteorites are spectrally linked to orbital observations on the scale of tens of meters is critical to understanding the development of igneous terrains on Mars, particularly the younger Amazonian volcanic provinces (e.g. Tharsis and Elysium).

Previously, visible and shortwave infrared (VSWIR) spectroscopy of powdered Martian meteorites has been conducted to characterize the spectral properties of Martian meteorites [e.g. 2,3,4], and select small point spectra has been used to nondestructively identify spectrally active phases that may be obscured in bulk powder spectra [e.g. 5,6]. While source craters for the Martian meteorites remain elusive, both powder and point spectra have been linked to remotely acquired spectra [e.g. 7,8] allowing greater utilization of petrologic and geochemical information from the Martian meteorites. However, with few examples of individual bulk powder or point spectra for each meteorite, the spectral diversity of grain-scale features may not be fully characterized.

Microimaging spectroscopy is an alternative technique recently applied to Martian meteorites [9,10] that can rapidly acquire tens of thousands of independent spectra on a spatial scale of microns, with minimal sample preparation. This technique has been demonstrated to be a powerful tool for extracting information about the mineralogy present in Martian meteorites [9]. Application of this technique to a large suite of Martian meteorites suggests that Martian meteorites may be visually sorted into distinct spectral classes based on 3-band false-color composites of the SWIR images collected for each meteorite [10]. This study builds on [10] by conducting a statistical analysis on the SWIR hyperspectral images of the suite of 52 Martian meteorites and investigating the petrologic significance of the statistically classified endmember spectra for different groups of Martian meteorites.

Methods: Previously acquired image cubes of 52 Martian meteorites [10], collected in laboratory with a Headwall Photonics imaging spectrometer at Caltech, were used to conduct this investigation. Each spectral cube contains data from 0.87-2.6 μm (shortwave infrared) wavelengths, at spatial resolutions of 212 μm/pixel with spectral resolutions of 6 nm. The meteorites are cut samples, and include 2 chassignites, 6 nakhlites, 52 shergottites, and 1 polymict breccia.

To identify and characterize spectrally active components of the meteorite dataset, Principal Component Analysis (PCA) was performed. This multivariate technique is often used in remote sensing analyses to remap the original data into a new space, with axes representing the dataset's total variance, without prior knowledge of what characteristics of the spectra are important [11]. This analysis was conducted on the entire suite of spectral cubes by combining all the pixels from every image

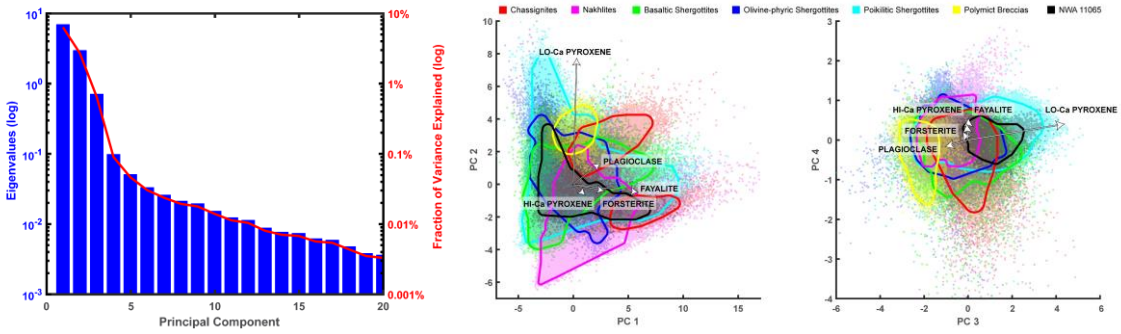

Figure 1. (L) Plot of the eigenvalues for principal components 1 through 20, as well as the percentage of variance explained by each principal component. (M,R) PCA biplots of the Martian meteorite classes. Line length for each library spectrum transformed into eigenvector coordinate axes is proportional to its importance in accounting for the data variance within each principal component. Principal components 1 and 2 (middle) and principal components 3 and 4 (right).

into a single dataset. For each pixel, the first five channels were masked due to noise in the data. Each pixel was then normalized at 1.607 μm to decrease the influence of albedo on the PCA. Finally, the mean channel value for each wavelength was subtracted. PCA was then calculated using a covariance matrix, and the data were recast along the principal component axes.

The meteorite dataset was also compared to library spectra from the PDS Geosciences Spectral Library, including spectra of forsterite, fayalite, low-Ca pyroxene, high-Ca pyroxene, and plagioclase measured at the NASA Reflectance Experiment Laboratory (RELAB) at Brown University. These library spectra were transformed into the principal component feature-space for direct comparison of the spectra with the meteorite data.

Results: With 279 wavelengths, 279 principal components were determined for the meteorite dataset. The first three eigenvectors contain 96.21% of the variance in the meteorite dataset, and the first fifteen eigenvectors contain 99.05% of the variance (Fig. 1).

PCA biplots were constructed for the first four principal components to determine how strongly each library spectrum influences a principal component (Fig. 1). In general, the shergottite meteorites (particularly the basaltic and poikilitic shergottites) have the highest variance in PC-space, likely due to their abundance in our dataset. Conversely, the polymict breccia has the least variance, representing a single sample, in spite of its lithological heterogeneity (NWA 11220). Two chassignite samples were analyzed (Chassigny and (NWA 2737), and these two samples plot in two distinct clusters. Based on the vector lengths for each library spectrum on the biplots, the low-calcium pyroxene appears to be tracked in PC2 and PC3, while olivine is weakly correlated with PC1. Plagioclase also appears to be anti-correlated with PC3, and has some influence on PC1 and PC2.

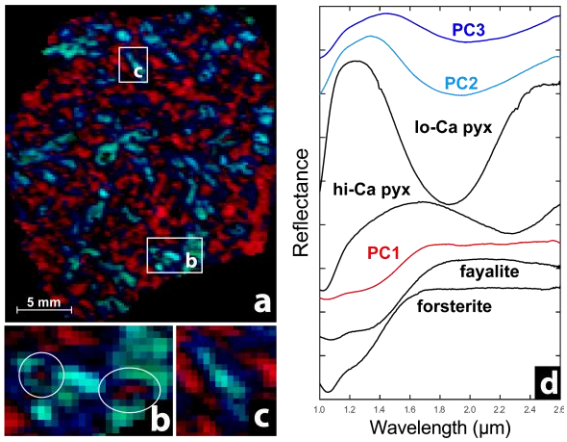

Figure 2. (a) False-color image of NWA. PC1 (red), PC2 (green), and PC3 (blue) result in olivines appearing red, low-Calcium pyroxene appearing cyan, and high-Calcium pyroxene appearing blue. (b) Inset illustrating two red olivine chadacrysts in pyroxene oikocrysts. (c) Inset demonstrating clear zoning between low-Ca core (cyan) and high-Ca rim (blue). (d) Average spectra for first three PCs alongside library spectra.

These relationships are highlighted in intermediate poikilitic shergottite NWA 11065 (Fig. 2a; black in Fig. 1). Pixels with a high value for PC1 have an average spectrum with a broad absorption at 1.04 μm, which is most similar to the iron-rich olivine spectrum that exhibits a broader, more asymmetric absorption at shorter wavelengths than more magnesium-rich olivines. NWA 11065 is unusually ferroan (olivine grains Fo_{54-68}) [12], which is well represented in the spectra identified by PC1. Although olivine chadacrysts are mostly absent in NWA 11065, PC1 identifies several pixels containing olivine oikocrystically enclosed by pyroxene.

Pixels with a high value for PC2 have an average spectrum with an absorption near 1 μm and a broader absorption of almost equal strength at 1.93 μm, which is most similar to the low-calcium pyroxene spectrum. Pixels with a high PC3 include both low-Ca pyroxenes and high-Ca pyroxenes; the average spectrum for pixels with a high value for PC3 but lower values for PC2 has am absorption near 1 μm and a broader absorption at 1.97 μm. In the image, these pixels surround the pixels identified as low-Ca pyroxene, representing the abrupt compositional boundaries between low-Ca cores and high-Ca rims. Pixels with a high value at PC4 appear to be correlated to a higher albedo near the normalization wavelength

Future Work: This study represents the first steps in understanding the spectrally active characteristics of different Martian meteorite classes, which can be linked to the spectral properties of surface-exposed igneous units on Mars. Future analysis will seek to develop a spectral classification of the Martian meteorites, characterize primary and secondary mineralogy within and between Martian meteorite classes, and determine the petrologic significance of spectral features.

Acknowledgements: Thanks to E. Stolper and J. Beckett (Caltech), M. Wadhwa (ASU), the Smithsonian Institute, and the University of Alberta for sample loans.

References: [1] McSween H. Y. (2015) *Am. Mineralogist* [2] Gaffey M. J. (1976) *JGR* [3] Bishop J. L. et al. (1998) *Met. Planet Sci.* 33 [4] Pieters C. M. et al. (2008) *JGR* [5] Schade U. & Wäsch R. (1999) *Met. Planet. Sci.* 34 [6] Palomba E. et al. (2006) *Icarus*, 182 [7] Lang N. P. et al. (2009) *JG*, 185 [8] Ody A. et al. (2015) *Icarus*, 258 [9] De Angelis S. et al. (2016) *LPSC XLVI*, Abstract #1223. [10] Cutts E. M. et al. (2018) *LPSC XLIV*, Abstract # 2749 [11] Mustard J. F. & Sunshine J. M. (1999) *Manual of Remote Sensing* [12] Rahib R. R. et al. (2019) *Geochim. Cosmochim. Acta*, 266